2013

Structurally diverse hamigerans from the New Zealand marine sponge Hamigera tarangaensis: NMR-directed isolation, structure elucidation and antifungal activity

A. Jonathan Singh

Jonathan D. Dattelbaum
University of Richmond, jdattelb@richmond.edu

Jessica J. Field

Zlatka Smart

Ethan F. Woolly

See next page for additional authors

Recommended Citation

Singh, A. Jonathan, Jonathan D. Dattelbaum, Jessica J. Field, Zlatka Smart, Ethan F. Woolly, Jacqueline M. Barber, Rosemary Heathcott, John H. Miller, and Peter T. Northcote. "Structurally Diverse Hamigerans from the New Zealand Marine Sponge Hamigera Tarangaensis: NMR-directed Isolation, Structure Elucidation and Antifungal Activity." *Organic & Biomolecular Chemistry* 11, no. 46 (2013): 8041-051. doi:10.1039/c3ob41305e.

Organic & Biomolecular Chemistry

RSC Publishing

Cite this: *Org. Biomol. Chem.*, 2013, **11**, 8041

Structurally diverse hamigerans from the New Zealand marine sponge *Hamigera tarangaensis*: NMR-directed isolation, structure elucidation and antifungal activity†

A. Jonathan Singh,[a] Jonathan D. Dattelbaum,‡[b] Jessica J. Field,[a] Zlatka Smart,[a] Ethan F. Woolly,[a] Jacqueline M. Barber,[a] Rosemary Heathcott,[a] John H. Miller[a] and Peter T. Northcote*[a]

Received 25th June 2013,
Accepted 29th July 2013

DOI: 10.1039/c3ob41305e

www.rsc.org/obc

The NMR-directed investigation of the New Zealand marine sponge *Hamigera tarangaensis* has afforded ten new compounds of the hamigeran family, and a new 13-*epi*-verrucosane congener. Notably, hamigeran F (**6**) possesses an unusual carbon–carbon bond between C-12 and C-13, creating an unprecedented skeleton within this class. In particular, the structural features of **6**, hamigeran H (**10**) and hamigeran J (**12**) imply a diterpenoid origin, which has allowed the putative biogenesis of three hamigeran carbon skeletons to be proposed based on geranyl geranyl pyrophosphate. All new hamigerans exhibited micromolar activity towards the HL-60 promyelocytic leukaemic cell line, and hamigeran G also selectively displayed antifungal activity in the budding yeast *Saccharomyces cerevisiae*. Homozygous deletion profiling (HOP) analysis suggests Golgi apparatus function as a potential target of this unusual class of sponge-derived terpenoids.

Introduction

Hamigera tarangaensis (Bergquist and Fromont, 1988) is a poecilosclerid sponge found predominately around northern New Zealand. The live sponge is orange-red to bright yellow underwater with rippled exterior and large, tented oscules. The first reported chemical study of *H. tarangaensis*, collected from the Hen and Chicken Islands off the northeastern coast of the North Island of New Zealand, resulted in the purported isolation of bromocyclooctane **1**.[1] Further examination of the sponge identified the hamigerans—phenolic compounds with varying degrees of bromination and cyclization.[2] The structures of the hamigerans were elucidated by NMR and X-ray methods,[3] which prompted the structural revision of **1** to hamigeran E (**5**). The reported biological activity of these compounds range from mild cytotoxicity (P388 murine leukaemia cells) to inhibition of herpes and polio viruses for hamigeran B (**4**). The tricarbocyclic skeleton and reported biological activity of the hamigerans, in particular **4**, has generated interest from synthetic organic chemists using a variety of approaches.[4–14]

Our work focused on a bright yellow sponge collected from Cape Karikari in coastal waters off the northern North Island of New Zealand that was subjected to an NMR-based screening protocol and examined for the presence of secondary metabolites. Analysis of ^{1}H and HSQC NMR spectra of the semi-purified extracts acquired in CD_3OD immediately presented a combination of interesting signals, including aromatic protons (δ_H 6.50–7.00, δ_C 120–130), deshielded methyl singlets (δ_H 2.00–2.50, δ_C 20–25) and highly shielded methyl doublets (δ_H 0.00–1.00, δ_C 20–25). In addition to these signals, proton resonances in the δ_H 10.00–14.00 range were observed when the ^{1}H NMR spectra of the screening fractions were acquired in $CDCl_3$, indicative of hydrogen-bound exchangeables. Acid digestion (HNO_3) of the sponge material and examination of the spicules (see ESI†) revealed unusually large, arcuate isochelae (average length: 52 μm) and strongyles (average dimensions: 357 × 7 μm) that matched the literature description for *H. tarangaensis*.[15] These data were correlated to the papers published by Cambie and co-workers which revealed the hamigerans as the isolates present in this sponge. The combination of NMR resonances mentioned above are consistent with those proposed for this class of compounds. The use of conventional isolation procedures, including size-exclusion chromatography and C18 HPLC, led to the isolation of three known and eight new members of the hamigeran family of compounds and a

[a]*Centre for Biodiscovery, Victoria University of Wellington, Wellington, New Zealand. E-mail: peter.northcote@vuw.ac.nz; Tel: +64 4 463 5960; Fax: +64 4 463 5237*
[b]*Department of Chemistry, University of Richmond, Richmond, VA 23173, USA*

†Electronic supplementary information (ESI) available: Isolation schemes, an extended proposed biogenesis and ^{1}H and ^{13}C NMR spectra for compounds **2–4**. Full 1D- and 2D-NMR data and spectra for compounds **6–8** and **10–19**. See DOI: 10.1039/c3ob41305e

‡J.D.D. was a visiting scholar to Victoria University of Wellington.

new 13-*epi*-neoverrucosane. Examination of a geographical variant of this sponge using EtOH in place of MeOH afforded an additional two new hamigeran congeners and an ethylated version of hamigeran A. The nature of these new hamigerans shed light on the biogenesis of this structural class.

Results/discussion

Isolation and structure determination

Methanolic extracts of a Cape Karikari specimen of *H. tarangaensis* were separated using a series of reversed-phase techniques (PSDVB, Me_2CO–H_2O, MeOH–0.1 M $HCOOH_{(aq)}$) and LH-20 size-exclusion chromatography. Final HPLC purification (C18, MeOH or MeCN–0.1–0.2 M $HCOOH_{(aq)}$) afforded new compounds **6**, **8**, **10–12** and **15–17** alongside the known compounds hamigeran A (**2**),[16] debromohamigeran A (**3**) and hamigeran B (**4**), with **2** and **4** prevalent in most fractions. A separate extraction of sponge material from Cavalli Island, with EtOH replacing all instances of MeOH in the isolation procedure, resulted in the isolation of compounds **13**, **14** and the ethyl ester variant of hamigeran A (as compound **19**) alongside smaller quantities of the known methyl ester **2** (Chart 1).

Hamigeran F (**6**) was isolated as a colourless film. The positive ion HRESIMS for hamigeran F showed a pseudomolecular $[M + Na]^+$ ion at *m*/*z* 459.0781 (Δ = −0.4 ppm), giving a molecular formula of $C_{21}H_{25}O_5Br$ with nine degrees of unsaturation. Evidence of bromine came in the form of an equally intense $[M + 2 + Na]^+$ peak. The ^1H, ^{13}C and multiplicity-edited HSQC NMR spectra in $CDCl_3$ (Table 1) revealed that 23 of the

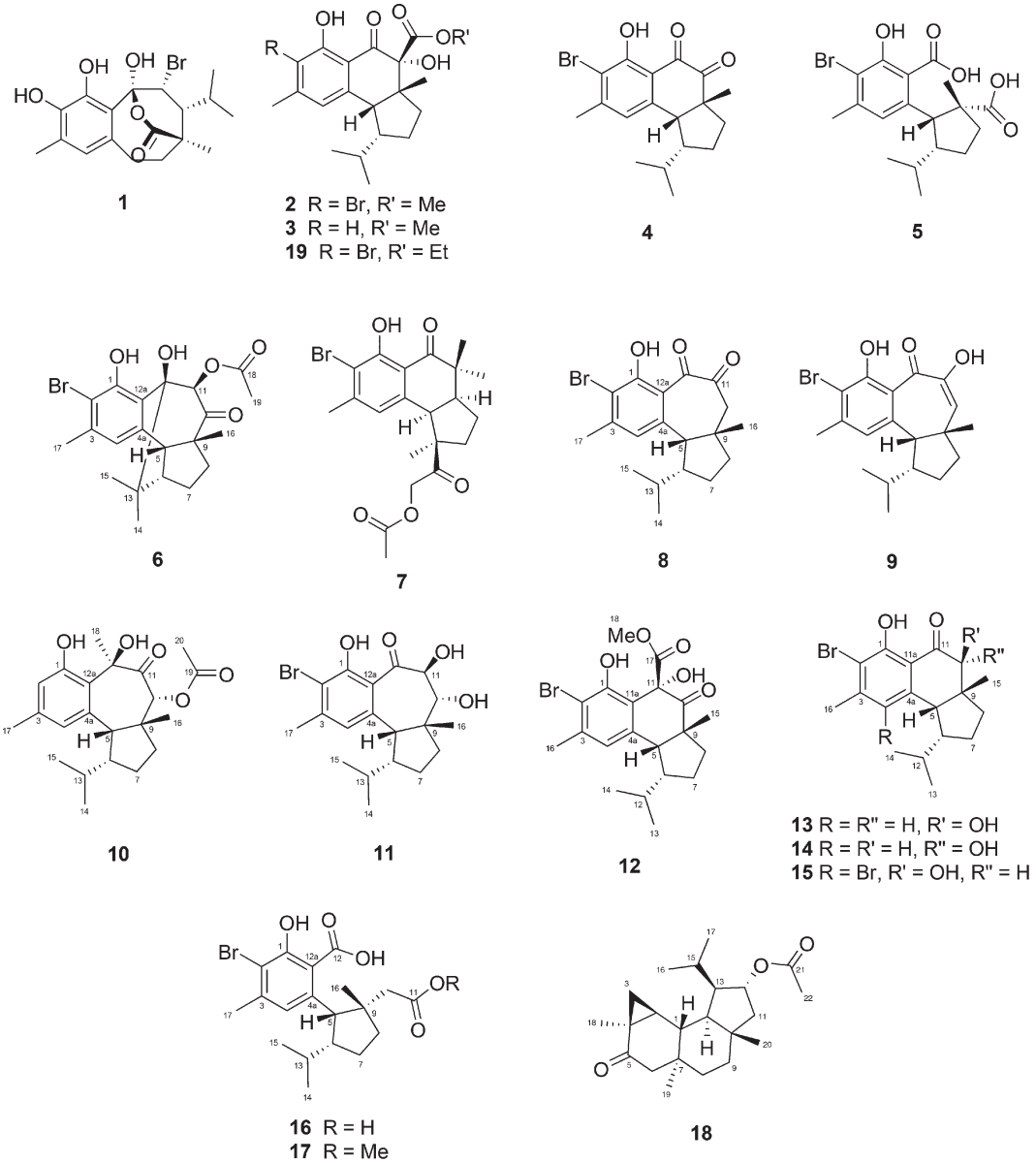

Chart 1

Table 1 ^{13}C (150 MHz) and ^{1}H (600 MHz) NMR data for hamigeran F (**6**) in $CDCl_3$

^{13}C				^{1}H				
Position	δ_C	mult.	$^{1}J_{CH}$ (Hz)	δ_H	mult. (J, Hz)	COSY	HMBC	NOESY
1	152.2	C						
1-OH				8.97	br s		1(w), 2(w), 12a(w)	
2	113.3	C						
3	138.8	C						
4	121.8	CH	160	6.52	s	5(w), 17	1(w), 2, 3(w), 4a(w), 5, 12(w), 12a, 17	5, 16, 17
4a	135.0	C						
5	53.9	CH	134	2.90	d (8.4)	4(w), 6	1(w), 4, 4a, 6, 9, 10, 12a, 13, 16	4, 6, 7(w), 8a(w), 15(w), 16
6	47.4	CH	135	2.41	td (8.7, 3.8)	5, 7	5, 8(w), 9, 12(w), 13	5, 7, 14, 15
7	27.9	CH_2	129	2.13	m	6, 8a, 8b	8(w), 9(w), 13	5(w), 6, 8a, 8b, 11, 14
8	36.5	CH_2	130[a]	1.75	m	7, 8b	6(w), 7(w), 9, 10(w), 16(w)	5(w), 7, 8b, 16
			133[a]	2.00	ddd (14.5, 8.1, 6.7)	7, 8a	5, 6, 10	7, 8a, 11, 14(w), 16(w)
9	58.3	C						
10	202.9	C						
11	79.3	CH	145	5.71	s		10, 12, 12a, 13, 18	7, 8b, 14
12	81.0	C						
12-OH				3.76	br s		12(w), 12a(w), 13(w)	
12a	119.6	C						
13	42.2	C						
14	20.0	CH_3	127	1.28	s	15	6, 12, 13, 15	6, 7, 8b(w), 11, 15
15	28.8	CH_3	127	0.81	s	14	6, 12, 13, 14	5(w), 6, 14
16	22.3	CH_3	126	1.13	s		5, 8, 9, 10	4, 5, 8a, 8b(w)
17	23.3	CH_3	128	2.33	s	4	2, 3, 4, 12a	4
18	171.6	C						
19	21.0	CH_3	130	2.22	s		11(w), 18	

[a] Estimated value due to distorted overlap.

25 protons were attached to 11 carbons, including: five methyls (δ_C 28.8; 23.3; 22.3; 21.0; 20.0), two methylenes (δ_C 36.5; 27.9) and four methines (δ_C 121.8; 79.3; 53.9; 47.4). The remaining ten carbons were assigned as non-protonated centres and included a ketone carbonyl (δ_C 202.9), an ester/lactone carbonyl (δ_C 171.6), five olefinic/aromatic carbons (δ_C 152.2; 138.8; 135.0; 119.6; 113.3) and three sp^3 quaternary carbons (δ_C 81.0; 58.3; 42.2). The nature of the five non-protonated aromatic carbons and the lone aromatic methine were consistent with the same phenolic moiety present in the known hamigerans. The two remaining protons (δ_H 8.97; 3.76) observed in the ^{1}H NMR experiment were assigned as exchangeable. With the evidence towards an aromatic ring and two carbonyl centres, the remainder of the structure must contain an additional three rings.

Further analysis of the 1D- and 2D-NMR data (Table 1) led to the identification of three spin systems. The lone aromatic methine (δ_C 6.52, δ_C 121.8, CH-4) and aromatic methyl (δ_C 2.33, δ_C 23.3, CH_3-17) were indicative of a pentasubstituted benzene ring that was established through COSY and HMBC correlations. The remainder of the structure was assigned through COSY and HMBC correlations (Fig. 1) and chemical shift comparisons with known hamigerans. The most significant change in this structure was the presence of a *gem*-dimethyl group (δ_C 42.2, C-13; δ_H 1.28, δ_C 20.0, CH_3-14; δ_H 0.81, δ_C 28.8, CH_3-15) in place of the usual isopropyl terminus—a new feature to this family of compounds. The *gem*-dimethyl moiety formed part of a fourth carbocyclic ring, as evidenced through a series of HMBC correlations to C-6 (δ_C 47.4) and C-12 (δ_C 81.0). NOESY correlations

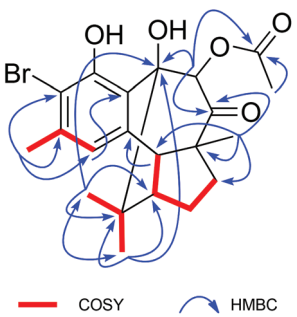

Fig. 1 Key COSY and HMBC correlations establishing the planar structure of hamigeran F (**6**).

between H-5, H-6 and H_3-16 indicated the retention of relative stereochemistry at these centres as observed in all other hamigeran congeners. Additional correlations between H-11 (δ_H 5.71) and H_3-14 placed these two groups on the same face of the molecule (Fig. 2). These data present hamigeran F as a new compound featuring a benzotricyclo[5.3.1.$0^{4,8}$]-undecane core, a new feature in this family of compounds and to our knowledge, an unprecedented natural product skeleton.

Prolonged storage of **6** in $CDCl_3$ led to the rearranged product **7**. The structure was assigned by direct comparison with **6**. The presence of a new, isolated oxymethylene (δ_H 4.11, 4.73; δ_C 67.0, CH_2-11) along with a new phenolic hydroxyl proton (δ_H 12.98, 1-OH) indicated a disconnection about the C-11 to C-12 bond. A second ketone carbonyl resonance at δ_C 209.1, corresponding to C-12, gave further evidence towards

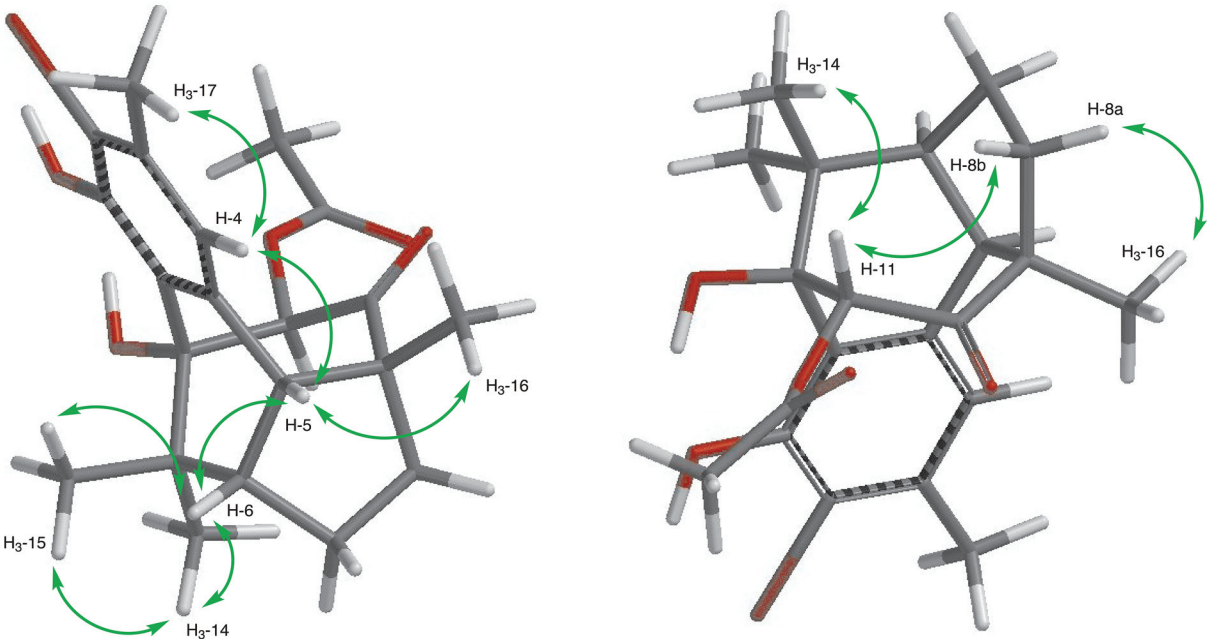

Fig. 2 Key NOESY correlations establishing the relative stereochemistry of hamigeran F (**6**).

the change in structure. We propose that the formation of **7** from **6** is due to an acid-catalyzed retro-aldol conversion, leading to cleavage of the C-11/C-12 σ-bond.

Hamigeran G (**8**), a pale-yellow amorphous solid, was assigned a molecular formula of $C_{19}H_{23}O_3Br$ (HRESIMS, $[M + Na]^+$, *m/z* 401.0731, Δ = +1.5 ppm). All 1D- and 2D-NMR spectra performed in $CDCl_3$ consistently showed two sets of resonances, despite exhaustive attempts at normal- and reversed-phase purifications. Additionally, evidence of conformational exchange between the two species was observed in the 2D NOESY of **8**, suggestive of two solution conformers. All 19 carbon resonances of the major conformer of hamigeran G were identified from analysis of the 1D- and 2D-NMR spectra (Table 2 and ESI†); 11 of which were confirmed through a multiplicity-edited HSQC as protonated centres: four methyls (δ_C 31.9; 24.2; 22.4; 22.2), three methylenes (δ_C 53.5; 40.7; 31.4) and four methines (δ_C 128.1; 60.8; 53.6; 29.9). The remaining eight non-protonated centres were assigned across two carbonyls (δ_C 195.8; 190.8), five aromatic carbons (δ_C 160.4; 148.3; 141.9; 118.6; 113.2) and one sp^3 quaternary carbon (δ_C 45.4). This required the one hydrogen at δ_H 12.18 to be attached to oxygen. Structure elucidation of the major compound followed closely to other hamigeran congeners, with the pentasubstituted aromatic ring, isopropyl side-chain and angular methyl all present in this structure. The key difference in this compound was the inclusion of an isolated methylene unit (δ_H 2.58, 2.71; δ_C 53.5, C-10) adjacent to a 1,2-diketone moiety at C-11 (δ_C 195.8) and C-12 (δ_C 190.8).

Assignment of the relative configuration of hamigeran G was achieved by analysis of ^1H–^1H coupling constants, NOESY data and comparison with other hamigerans. With only three centres to consider—C-5, C-6 and C-9—the assignments were relatively simple to make. NOESY correlations between H-5 and H_3-16 indicated the retention of the *cis*-fusion of the bicyclo[5.3.0]decane. H-5 (d, 11.3 Hz) also correlated in this fashion to H-6, suggestive of conserved relative stereochemistry at these centres between **8** and other known hamigerans. It is thought that the presence of a minor conformer of **8** is due to the conformational flux of this diketone unit. In addition, hamigeran G (**8**) also tautomerizes to the diosphenol **9**, which could be separated using reversed-phase HPLC and studied with NMR (see ESI†) long enough to obtain data before reverting back to the diketo compound **8**.

Hamigeran H (**10**) was isolated as a pale yellow/colourless film. The molecular formula of $C_{22}H_{30}O_5$ was determined through HRESIMS ($[M + Na]^+$, *m/z* 397.1995, Δ = +1.0 ppm). All 22 carbons and 30 protons were observed in the respective ^{13}C and ^1H NMR spectra (Table 2 and ESI†), consistent with the proposed molecular formula. The multiplicity-edited HSQC experiment showed 14 protonated carbons, belonging to six methyls (δ_C 30.0; 23.6; 22.0; 21.5; 20.9; 20.8), two methylenes (δ_C 34.2; 31.3) and six methines (δ_C 129.4; 119.3; 80.0; 61.5; 53.1; 27.7). Of the remaining eight non-protonated carbons, two were assigned as carbonyls (δ_C 202.9; 172.7), four aromatic carbons (δ_C 158.4; 138.8; 135.0; 123.1), and two quaternary sp^3 centres (δ_C 80.3; 47.9). In comparison to the previously reported hamigerans, a tertiary methyl (δ_H 1.81, δ_C 22.0, CH_3-18), an additional aromatic methine (δ_H 6.76, δ_C 119.3, CH-2) and a saturated ketone at δ_C 202.9 stood out as the most notable features of this compound. Construction of the planar structure of **10** was made in the same fashion as the previous compounds, with the placement of CH_3-18 established by way of HMBC correlations to C-11, carbinol C-12 (δ_C 80.3), C-12a, and a COSY correlation with 12-OH (δ_H 4.70).

Table 2 ^{1}H (600 MHz) and ^{13}C (150 MHz) NMR data for isohamigerane-derived compounds **8**, **10**, **11**, **16**, and **17** in $CDCl_3$

	8[a]		**10**		**11**		**16**		**17**	
Position	δ_C mult.	δ_H mult. (J, Hz)	δ_C mult.	δ_H mult. (J, Hz)	δ_C mult.	δ_H mult. (J, Hz)	δ_C mult.	δ_H mult. (J, Hz)	δ_C mult.	δ_H mult. (J, Hz)
1	160.4 C		158.4 C		160.9 C		159.0 C		156.7 C	
1-OH		12.18 s		8.84 s		13.30 s				
2	113.2 C		119.3 CH	6.76 d (1.2)	113.6 C		112.3 C		111.8 C	
3	148.3 C		138.8 C		148.2 C		144.6 C		143.4 C	
4	128.1 CH	6.78 s	129.4 CH	6.55 s	128.4 CH	6.77 s	123.6 CH	6.56 s	123.2 CH	6.53 s
4a	141.9 C		135.0 C		141.9 C		144.2 C		141.7 C	
5	60.8 CH	3.39 d (11.3)	61.5 CH	3.51 d (11.4)	61.2 CH	3.44 d (11.7)	50.1 CH	4.55 d (6.9)	52.9 CH	3.87 d (7.2)
6	53.6 CH	2.01 m	53.1 CH	1.90 m	53.9 CH	2.22 m	51.6 CH	2.34 m	51.7 CH	2.23 m
7	31.4 CH_2	1.16 qd (13.0, 6.5)	31.3 CH_2	1.11 qd (13.0, 6.3)	32.5 CH_2	1.58 m	28.8 CH_2	1.64 m	29.1 CH_2	1.64 m
		1.74 m		1.59 m		1.92 dddd (16.3, 13.9, 8.1, 2.6)		2.16 m		2.08 m
8	40.7 CH_2	1.62 td (13.2, 6.7)	34.2 CH_2	1.28 m	34.6 CH_2	1.42 m	38.7 CH_2	1.57 ddd (12.4, 9.9, 2.1)	37.9 CH_2	1.78 m
		1.98 m		2.27 m		2.57 ddd (13.6, 7.2, 2.5)		1.77 td (12.5, 7.5)		1.92 m
9	45.4 C		47.9 C		47.9 C		47.2 C		46.2 C	
10	53.5 CH_2	2.58 d (12.0)	80.0 CH	5.15 s	74.45[b] CH	3.32 d (10.8)	42.4 CH_2	1.83 d (15.5)	43.4 CH_2	2.02 d (15.1)
		2.71 d (12.0)						2.06 d (15.3)		2.38 d (15.1)
10-OH						4.15 br s				
11	195.8 C		202.9 C		74.43[b] CH	4.59 d (10.8)	180.0 C		174.8 C	
11-OH						3.17 br s				
12	190.8 C		80.3 C		204.9 C		177.3 C		172.1 C	
12-OH				4.70 s						
12a	118.6 C		123.1 C		116.3 C		113.1 C		115.4 C	
13	29.9 CH	0.84 m	27.7 CH	0.96 m	29.6 CH	1.10 m	30.7 CH	1.40 m	30.1 CH	1.12 m
14	22.2 CH_3	0.69 d (6.5)	21.5 CH_3	0.70 d (6.3)	22.1 CH_3	0.77 d (6.6)	22.5 CH_3	0.91 d (6.5)	22.3 CH_3	0.82 d (6.5)
15	22.4 CH_3	0.25 d (6.5)	23.6 CH_3	0.61 d (6.8)	23.5 CH_3	0.20 d (6.1)	22.0 CH_3	0.69 d (6.4)	22.2 CH_3	0.63 d (6.4)
16	31.9 CH_3	1.29 s	30.0 CH_3	1.30 s	30.1 CH_3	1.25 s	27.7 CH_3	1.31 s	28.2 CH_3	1.25 s
17	24.2 CH_3	2.48 s	20.9 CH_3	2.26 s	24.0 CH_3	2.45 s	24.6 CH_3	2.45 s	24.5 CH_3	2.43 s
18			22.0 CH_3	1.81 s					51.9 CH_3	3.59 s
19			172.7 C							
20			20.8 CH_3	2.16 s						

[a] Major conformer. [b] Interchangeable.

The completed planar structure of hamigeran H (**10**) contains five stereogenic centres. Diagnostic NOESY correlations between H-5, H-6 and H_3-16 indicated retention of the relative stereochemistry of these centres, consistent with the other hamigeran compounds. These conserved correlations also established the relationship of the two new stereocentres CH-10 and C-12, leading to the relative stereochemistry shown. Through-space correlations observed between H-10 and H_3-16 implies a *cis* relationship and places H-10 on the same (convex) face as H-5 and H-6. For C-12, a set of NOESY correlations between methyl H_3-18 and the C-13–C-15 isopropyl group means that they occupy the concave face.

The molecular formula of hamigeran I (**11**) was established as $C_{19}H_{25}O_4Br$ through analysis of its $[M + Na]^+$ pseudomolecular ion (HRESIMS, m/z 419.0837, Δ = +0.7 ppm). NMR evidence of all 19 carbons and 25 protons (Table 2 and ESI†) led to the planar structure with a hydrogen-bonded phenolic hydroxyl proton at δ_H 13.30 and an α,β-unsaturated ketone (δ_C 204.9) among the diagnostic features for this compound. With the majority of the constitutional structure of **11** being similar to other congeners, the most relevant structural aspect of this compound was the vicinal diol occupied by positions CH-10 (δ_H 3.32, δ_C 74.45) and CH-11 (δ_H 4.59, δ_C 74.43). In assigning the relative stereochemistry of **11**, a set of NOESY correlations between H-5, H-6 and H_3-16 validated the typically observed *cis*-fusion of the bicyclo[5.3.0]decane and orientation of the isopropyl group. The *trans* relationship between H-10 and H-11 was established by vicinal coupling constants ($^3J_{HH}$ = 10.8 Hz) and supported by respective NOESY correlations between H-10 and H_3-16, and H-11 with H-13.

Hamigeran J (**12**), with a molecular formula of $C_{20}H_{25}O_5Br$ (HRESIMS, $[M + Na]^+$, m/z 447.0786, Δ = +0.7 ppm), is isomeric with hamigeran A (**2**). At first glance, spectroscopic data for **12** strongly resembled that of hamigeran A (**2**). Evidence of a methyl ester (δ_C 170.6, C-17; δ_H 3.74, δ_C 53.8, CH_3-18) and the observation that most of the ^{13}C and ^{1}H NMR chemical shifts (Table 3 and ESI†) were in close match with **2** confirmed this assumption and allowed most of the structure to be assigned through direct comparison. However, the absence of an ^{1}H NMR resonance attributed to a hydrogen-bonded phenolic proton and an HMBC correlation from CH_3-16 (δ_H 1.31) to a signal at δ_C 210.1 (C-10) placed a saturated ketone adjacent to the tertiary methyl, rather than an α,β-unsaturated ketone adjacent to the aromatic ring as observed in **2** (δ_C 198.1, C-12). NOESY correlations observed between H-5, H-6 and H_3-15, along with a diagnostic through-space correlation between H_3-15 and H_3-18, confirms that hamigeran J (**12**) is a regioisomer of hamigeran A (**2**).

Hamigeran K (**13**, $C_{18}H_{23}O_3Br$), 10-*epi*-hamigeran K (**14**, $C_{18}H_{23}O_3Br$) and 4-bromohamigeran K (**15**, $C_{18}H_{22}O_3Br_2$)

Table 3 ^{1}H (600 MHz) and ^{13}C (150 MHz) NMR data for hamigerane-derived compounds **12–15**

	12		**13**		**14**		**15**	
Position	δ_C mult.	δ_H mult. (J, Hz)	δ_C mult.	δ_H mult. (J, Hz)	δ_C mult.	δ_H mult. (J, Hz)	δ_C mult.	δ_H mult. (J, Hz)
1	151.8 C		158.1 C		156.6 C		157.8 C	
1-OH				12.22 s		11.63 s		12.62 s
2	112.0 C		110.8 C		110.8 C		112.7 C	
3	139.7 C		148.1 C		147.3 C		148.2 C	
4	125.0 CH	6.78 s	124.5 CH	6.66 s	123.1 CH	6.73 s	119.3 C	
4a	136.6 C		142.4 C		140.2 C		142.7 C	
5	57.0 CH	3.34 d (9.0)	52.2 CH	3.13 d (12.3)	50.5 CH	3.20 d (6.1)	54.9 CH	3.33 d (12.2)
6	51.2 CH	2.16 tt (14.0, 7.4)	48.0 CH	2.64 m	53.6 CH	2.01 m	46.4 CH	2.93 m
7	27.4[a] CH_2	1.62 m	24.8 CH_2	1.77 m	28.0 CH_2	0.71 m	24.2 CH_2	1.73 m
		1.72 m		1.86 m		1.66 m		1.92 m
8	35.6 CH_2	1.45 dt (13.2, 8.0)	36.0 CH_2	1.46 m	31.9 CH_2	1.36 m	36.0 CH_2	1.46 m
		2.56 ddd (13.3, 7.3, 6.2)		2.23 dd (13.1, 6.5)		1.64 m		2.25 m
9	55.2 C		50.4 C		44.5 C		50.6 C	
10	210.1 C		73.7 CH	4.43 s	78.1 CH	4.25 br s	73.0 CH	4.49 s
10-OH				3.47 br s		3.67 br s		
11	76.8 C		204.2 C		202.7 C		204.9 C	
11a	120.0 C		113.8 C		115.5 C		114.7 C	
12	27.5[a] CH	1.37 m	28.4 CH	1.81 m	26.9 CH	1.49 m	28.7 CH	1.66 m
13	20.1 CH_3	0.54 d (6.6)	23.6 CH_3	0.81 d (6.8)	23.6 CH_3	1.18 d (6.3)	23.5 CH_3	0.80 d (6.9)
14	23.4 CH_3	0.45 d (6.6)	17.7 CH_3	0.43 d (6.8)	21.9 CH_3	0.79 d (6.6)	18.1 CH_3	0.47 d (6.8)
15	25.9 CH_3	1.31 s	19.7 CH_3	1.00 s	28.6 CH_3	1.43 s	19.4 CH_3	0.98 s
16	23.6 CH_3	2.42 s	24.4 CH_3	2.46 s	24.6 CH_3	2.46 s	26.4 CH_3	2.73 s
17	170.6 C							
18	53.8 CH_3	3.74 s						

[a] Interchangeable.

were all identified as C-10 reduced forms of hamigeran B (**4**) and 4-bromohamigeran B, respectively, with the structures of all three compounds resolved by direct comparison with their parent compounds (Table 3 and ESI†). Analysis of the HRESIMS molecular ion clusters confirmed the presence of a single bromine in **13** and **14** ($[M + Na]^+$, m/z 389.0724/389.0726, Δ = −1.0/−0.5 ppm), and two bromine atoms in **15** ($[M + Na]^+$, m/z 466.9833, Δ = 0.0 ppm). For all three compounds, COSY and HMBC correlations established aromatic and aliphatic spin systems in accordance with the sequence observed for the (4-bromo)hamigeran B framework. The relative stereochemistry about the CH-10 oxymethine for compounds **13** and **15** were both established by long-range w-coupling between H-10 and H_3-15, indicative of a 1,2-diaxial relationship. By default, 10-*epi*-hamigeran K (**14**) was assigned the opposite relative stereochemistry for this position.

The molecular formulae for hamigeran L (**16**), $C_{19}H_{25}O_5Br$, and its methyl ester **17**, $C_{20}H_{27}O_5Br$, were both determined from HRESIMS ($[M + Na]^+$, m/z 435.0784 and 449.0933, respectively). Analysis of 1D- and 2D-NMR data for both compounds (Table 2 and ESI†) quickly led to the identification of their structures as homologues of hamigeran E (**5**). The two compounds mirrored hamigeran E in their planar structures, with the exception of an isolated, diastereotopic methylene centre at C-10. In the case of **17**, placement of the methyl ester was achieved by way of an HMBC correlation from H_3-18 (δ_H 3.59) to C-11 (δ_C 174.8). As hamigeran E can be rationalized as an oxidation product of hamigeran B (**4**), the corollary can be assumed with **16** and **17** to hamigeran G (**12**).

Taking into account the stereochemical features of the known hamigerans, for which the absolute configuration of hamigerans A and B have been verified by X-ray and total synthesis, assignment of absolute configuration for the new hamigeran structures reported in this study are implied as drawn. Specifically, the absolute configuration of hamigeran F (**6**) is proposed to be 5*R*,6*S*,9*R*,11*R*,12*S*.

In the process of isolating compounds **6–12**, a new, unrelated compound was isolated. 12-Acetoxy-13-*epi*-neoverrucosan-5-one (**18**), isolated as a colourless film, was identified with a molecular formula of $C_{22}H_{34}O_3$ (HRESIMS, $[M + Na]^+$, m/z 369.2401, Δ = −1.4 ppm). All 22 carbons and 34 protons were accounted for in the ^{1}H, ^{13}C and HSQC NMR spectra; whereas, evidence of the three oxygens was found in a saturated ketone at δ_C 211.4 and an acetate moiety (δ_H 2.05; δ_C 21.6, 170.6). The remaining four double bond equivalents were therefore satisfied through four rings. Standard elucidation procedures provided the planar structure of three rings, while an additional HSQC experiment, optimized for $^{1}J_{CH}$ = 170 Hz, enhanced one methylene and one methine unit that appeared weakly in the default experiment ($^{1}J_{CH}$ = 140 Hz). COSY evidence from these two centres and HMBC correlations from H_3-18 formed a structure consistent with a cyclopropane moiety, thereby satisfying the fourth unsaturation. With the planar structure of **18** complete, 1D- and 2D-NOESY experiments set the relative stereochemistry as shown. In $CDCl_3$, severe second-order effects observed between H-1 and H-14 prevented unequivocal proof of their direct connection and stereochemical relationship—only through changing solvents to C_6D_6 was a *trans* relationship observed ($^{3}J_{HH}$ ~ 12.0 Hz)

between the two centres. From these data, the structure of compound **18** was assigned as a 13-*epi*-neoverrucosane.

Proposed biogenesis

The original report of the hamigerans did not comment on the possible biogenetic origins of the compounds. The structures of hamigerans F (**6**), H (**10**) and J (**12**) are consistent with a diterpene precursor, which enables us to propose a biogenetic pathway previously lacking in the literature. If a terpenoid origin is considered, the hamigerans can be divided into two distinct carbon skeletons emanating from geranyl geranyl pyrophosphate (GGPP)—termed here as *hamigerane* and *isohamigerane* (Fig. 3), in which the B ring is a six- or seven-membered ring, respectively. In the case of hamigeran F (**6**), a third *neohamigerane* skeleton exists. All compounds derived from either skeleton are norditerpenoids (or bis-norditerpenoids as with **4**) with the exception of hamigeran H (**10**), which has its full complement of carbons. Structural features conserved throughout all hamigeran compounds are the phenol moiety, an unmodified cyclopentane, the *cis*-fusion of the B and C rings, the relative stereochemistry of C-10 and C-11 in the isohamigeranes, and the presence and orientation of the methyl esters in hamigerans A (**2**) and J (**12**). These are all significant markers when postulating a biogenetic pathway for these compounds.

Scheme 1 shows a proposed biogenetic pathway to the hamigerans from GGPP as the acyclic precursor. The carbon numbering system used here is based on GGPP and should not be confused with the system used for the final compounds. A series of allylic oxidations at C-5, C-8 and C-9, followed by an *E*/*Z*-isomerization would facilitate the formation of the aromatic A ring, while placing the phenolic hydroxyl group at the correct position (C-5). In this proposed biogenesis, the order of cyclization is important. If the cyclopentane ring is formed first, there is no allylic centre available for oxidation. A cascade cyclization forms the internal cyclohexyl B ring and cyclopentyl C ring, promoted by the capture of an electrophile (X), such as a proton or bromonium ion. Alternatively, the system is primed for a 6π disrotatory electrocyclic closure in which, while aromaticity is initially lost, the second cascade restores aromaticity and gives the same tricyclic product. Removal of pyrophosphate (OPP) from C-1 forms the relatively unstable primary carbocation that can be stabilised by delocalisation of the C-3/C-17 methylidene.[17] This can then rearrange *via* either 1,2-hydride or 1,2-alkyl shifts to give the hamigerane (pathway *a*) or isohamigerane (pathway *b*) carbon skeletons, respectively. A more detailed sequence is provided in the ESI.† The occurrence of both hamigeran A ethyl ester (**19**) and **2** from the EtOH extraction of *H. tarangaensis*, verified by ^{1}H NMR and LCMS evidence, is consistent with our proposed biogenesis and suggests the free acid is produced by the sponge, with **2**, **3** and possibly **12** existing as both artefacts of isolation and as naturally occurring compounds.

In order to rationalize the existence of the neohamigerane skeleton, a σ-bond must form between C-3 and C-15, which could be made possible through a number of pathways. Enzymatic abstraction of isopropyl methine H-15, performed in a manner similar to that required for the earlier cascade sequence, may provide a route to bond formation with the C-3 ketone. Alternatively, if the electrophile captured earlier in the sequence was a bromonium ion rather than a proton, bond formation could occur *via* a metal-initiated mechanism, *e.g.* an enzymatic Barbier-type reaction. The aforementioned oxidation of C-17 to a carboxylic acid and subsequent decarboxylation may also provide impetus for this unusual bond formation.

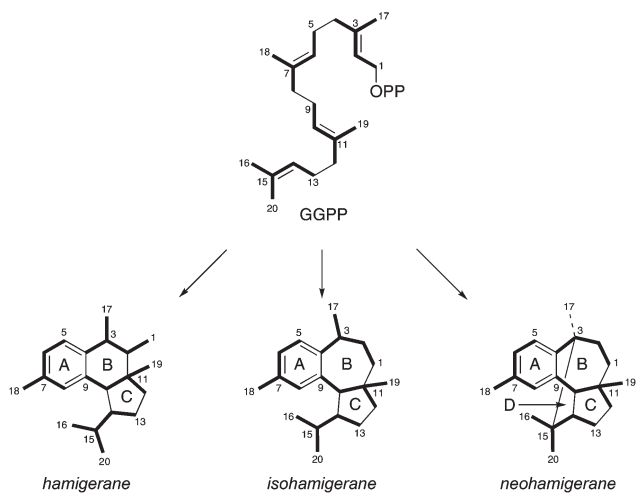

Fig. 3 Hamigeran skeletons derived from geranyl geranyl pyrophosphate (GGPP).

Biological activity

3-(4,5-Dimethylthiazol-2-yl)-2,5-diphenyltetrazolium bromide (MTT) cell proliferation assays revealed that hamigerans F–J were moderately cytotoxic towards the HL-60 (human promyelocytic leukaemic) cell line (Table 4). Hamigeran F (**6**) was among the more cytotoxic of these new compounds, with an IC_{50} value of 4.9 ± 1.2 μM; and its rearrangement product **7** was similar in potency (IC_{50} 7.4 ± 1.9 μM). Hamigeran G (**8**) exhibited the greatest cytotoxicity of these newly isolated compounds with an IC_{50} value of 2.5 ± 0.2 μM; whereas the potencies of compounds **10–17** ranged between 5.6–78.3 μM. The cytotoxicities of known compounds **2–4** obtained in this study correlate closely to those exhibited by the new compounds and are comparable to the values initially reported against the P388 cell line.[2] Hamigerans F–J were also tested in cell cycle arrest assays by flow cytometry, with all five compounds showing a slight increase of cell accumulation at the G_2/M checkpoint, indicative of an antimitotic action. 12-Acetoxy-13-*epi*-neoverrucosan-5-one (**18**) was ineffective towards HL-60 cell cycle progression at concentrations of up to 50 μM.

The level of cytotoxicity displayed by hamigeran G (**8**) in the MTT proliferation assay, coupled with access to enough of the natural product, led us to initiate further studies in other biological systems. Because of the ease of genetic manipulation and rapid turnover time in yeast, we tested hamigeran G for its

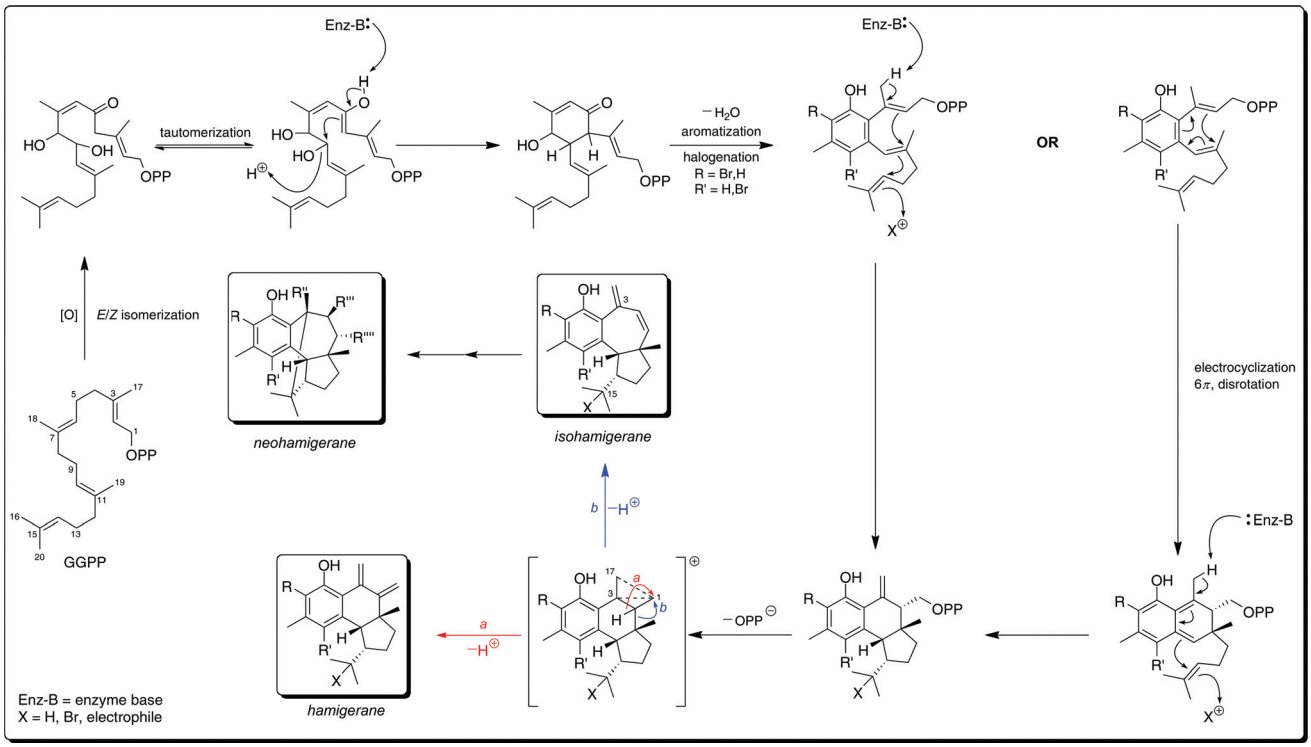

Scheme 1 Possible biogenesis of the hamigerane, isohamigerane and neohamigerane skeletons, derived from geranyl geranyl pyrophosphate (GGPP).

Table 4 Hamigeran IC_{50} values (HL-60, n = 3 replicates)

Compound	Mean IC_{50} ± SEM (μM)
Hamigeran A (**2**)	16.0 ± 4.5
Debromohamigeran A (**3**)	12.5 ± 3.4
Hamigeran B (**4**)	3.4 ± 0.4
Hamigeran F (**6**)	4.9 ± 1.2
Hamigeran F rearrangement product (**7**)	7.4 ± 1.9
Hamigeran G (**8**)	2.5 ± 0.2
Hamigeran H (**10**)	16.5 ± 1.4
Hamigeran I (**11**)	37.2 ± 1.4
Hamigeran J (**12**)	48.2 ± 1.2
Hamigeran K (**13**)	13.7 ± 0.6
10-*epi*-Hamigeran K (**14**)	28.5 ± 1.6
4-Bromohamigeran K (**15**)	5.6 ± 0.4
Hamigeran L (**16**)	78.3 ± 0.5
Hamigeran L 11-*O*-methyl ester (**17**)	21.1 ± 3.3

ability to inhibit the growth of the budding yeast *Saccharomyces cerevisiae*, as this would allow us to screen for genes involved in its mode of action.[18] Chemical genomic screens were carried out to gain insight into the genetic pathways involved in the growth inhibition by hamigeran G. We used a yeast strain deficient in drug efflux pumping activity to maximise the effect of hamigeran G in the cell. We also repeated the screen in a homozygous diploid yeast strain with normal efflux pump activities. Hamigeran G inhibited growth of both strains with IC_{50} values of 6.7 μM and 16.5 μM, respectively. For each screen, a pool of deletion mutants were grown in the presence of hamigeran G at a concentration that gave a 20% reduction in growth. We then identified individual deletion mutants for each non-essential gene that showed reduced growth, using a barcode microarray method as previously described.[19] The genes that were linked to hamigeran G were then analysed using Funspec (http://funspec.med.utoronto.ca/). Genes associated with the Golgi apparatus and Golgi vesicle transport of proteins were particularly highlighted in the interactive networks. Genes involved in vesicle-mediated transport included SNC1, SFT2, ARL1, GET3, SEC22, GYP1, RUD3; intra-Golgi vesicle-mediated transport included COG7, COG8, COG6, COG5; vesicle fusion included SNC1,GOS1, SEC22; Golgi to plasma membrane protein transport included ARL1, SYS1; ER to Golgi vesicle-mediated transport included GOS1, SEC22, RUD3. Of the 13 Golgi transport-related genes identified in the drug efflux pump knockout strains (1*n* screen), nine were also significant hits in the non-pump knockout, homozygous deletion strains (2*n* screen). In a single screen with the efflux pump knockout strain, hamigeran B (**4**), which showed little inhibitory activity on growth of this strain, was affected by deletion of only two of the 13 Golgi-related genes identified with hamigeran G, specifically RUD3 and SFT2. Our results suggest that hamigeran G may target the sorting and transport of proteins within the Golgi network of the cell.

Conclusion

An NMR-guided investigation of the New Zealand marine sponge *Hamigera tarangaensis* has resulted in the isolation of several structurally diverse hamigerans, from which a unified

diterpenoid biogenesis has been proposed. Hamigeran F (**6**), with its unusual tetracyclic core, may be an interesting synthetic target. The selective antifungal activity displayed in yeast by hamigeran G (**8**) is also intriguing. With access to larger quantities of known and new hamigerans, particularly hamigerans B (**4**) and G (**8**), further studies have been undertaken to decipher the mode of action of this family of compounds.

Experimental

General

NMR spectra were recorded using a Varian DirectDrive 600 MHz spectrometer, equipped with a HCN triple resonance cryogenic probe. Chemical shifts (δ, ppm) were referenced to the residual solvent peak.[20] High-resolution mass spectra were measured using a Waters Q-TOF Micromass Premier spectrometer. Optical rotations were measured using Rudolph Autopol II or Perkin-Elmer 241 polarimeters. UV spectra were recorded on a dual-beam spectrophotometer. HPLC was performed using a Varian PrepStar 210 solvent delivery module with 100 mL pump heads (preparative scale), or a Rainin Dynamax SD-200 solvent delivery system with 25 mL pump heads (semi-preparative and analytical scale). UV/vis detection for HPLC runs was obtained with a Varian Prostar 335 photodiode array detector. Solvents used for flash normal- and reversed-phase column chromatography are of HPLC or analytical grade quality. All other solvents were purified by distillation before use. Solvent mixtures are reported as % vol/vol unless otherwise stated.

Animal material

Sponges were collected by hand using SCUBA at Cape Karikari and Cavalli Island, New Zealand in 2003. Specimens were stored at −20 °C until extraction. Voucher samples are stored at the School of Chemical and Physical Sciences, Victoria University of Wellington. Spicule analysis using SEM and comparison with literature[21] concluded that the sponge was *H. tarangaensis*.

Extraction and isolation

Hamigeran F. Frozen *Hamigera tarangaensis* (PTN2_66E, 124.7 g), collected from Cape Karikari, New Zealand, was extracted twice with MeOH (400 mL). The second, then first extracts were loaded on an 80 mL HP20 column, pre-equilibrated in MeOH. The loaded column was then washed with 250 mL portions of (i) H_2O, (ii) 30% Me_2CO–H_2O (fraction A), (iii) 75% Me_2CO–H_2O (fraction B), and (iii) Me_2CO (fraction C). A 376.7 mg subsample of fraction B was fractionated on silica gel (70 mL), eluting with 200 mL portions of 50% hexanes–CH_2Cl_2 (fraction D), followed by EtOAc–CH_2Cl_2 (0–100%, fractions E1–172). Fractions E42–54 (1–2% EtOAc–CH_2Cl_2) were combined and loaded on to a 20 mL column of HP20SS and eluted with 60 mL portions of MeOH–H_2O (20–100%, fractions G–M). The 80–90% MeOH–H_2O fractions (K and L) were combined and purified using HPLC (C18, 90% MeOH–0.1 M $HCOOH_{(aq)}$), giving hamigeran F (**6**, t_R 7.3 min, 2.6 mg). The mixture of hamigeran F and its rearrangement product was separated by C18 HPLC (85% MeOH–0.2 M $HCOOH_{(aq)}$), which afforded the latter compound (**7**, t_R 12.0 min, 0.4 mg) as a colourless film.

Hamigerans G–J, 4-bromohamigeran K, hamigeran L, hamigeran L 11-*O*-methyl ester and 12-acetoxy-13-*epi*-neoverrucosan-5-one. A second, separate sample of *H. tarangaensis* (PTN2_66E, 266 g frozen weight) was cut into small pieces and extracted with MeOH (2 × 1.5 L) for 24 h. The second, then first extracts were passed through a 1 L column of HP20 PSDVB beads, pre-equilibrated in MeOH. The combined eluent was diluted with H_2O (3 L) and passed back through the column. This eluent was again diluted with H_2O (6 L) and passed again through the column. The loaded column was then washed with H_2O (3 L) followed by 3 L portions of (i) 20% Me_2CO–H_2O (fraction A), (ii) 40% Me_2CO–H_2O (fraction B), (iii) 60% Me_2CO–H_2O (fraction C), (iv) 80% Me_2CO–H_2O (fraction D), (v) Me_2CO (fraction E). A 600 mg portion of the 80% Me_2CO–H_2O fraction was loaded on to a 20 mL column of HP20SS PSDVB beads, placed on top of another HP20SS column (350 mL), and eluted with increasing concentrations of MeOH in 0.1 M $HCOOH_{(aq)}$ (75–100%). Thirty-eight fractions (100 mL each) were collected, and combined as follows: (i) 1–7 (fraction F), (ii) 8–12 (fraction G), (iii) 13–19 (fraction H), (iv) 20–22 (fraction I), (v) 23–27 (fraction J), and (vi) 28–38 (fraction K). Fraction G (56.2 mg) was subjected to C18 HPLC (75% MeOH–0.2 M $HCOOH_{(aq)}$), giving seven fractions (L–R). Fraction M (12.9 mg) was again subjected to C18 HPLC (65% MeCN–0.2 M $HCOOH_{(aq)}$), resulting in another ten fractions (S–AB), where fractions V and X gave hamigerans I (**11**, t_R 14.4 min, 0.4 mg) and J (**12**, t_R 16.5 min, 3.1 mg), respectively.

C18 HPLC (80% MeCN–0.2 M $HCOOH_{(aq)}$) purification of fraction N (7.6 mg) generated fractions AC–AF, from which fraction AD gave debromohamigeran A (**3**, t_R 10.1 min, 1.4 mg), while fraction AE afforded 12-acetoxy-13-*epi*-neoverrucosan-5-one (**18**, t_R 10.8 min, 1.9 mg). Fraction O (4.0 mg) was also purified further with C18 HPLC (70% MeCN–0.2 M $HCOOH_{(aq)}$), giving four fractions (AG–AJ), where fraction AH resulted in hamigeran H (**10**, t_R 16.0 min, 1.1 mg). Fraction K (111.7 mg) was further purified using HPLC (C18, 75% MeOH–0.2 M $HCOOH_{(aq)}$), affording ten fractions (AK–AT). Fractions AO and AQ gave hamigerans B (**4**, t_R 34.9 min, 14.3 mg) and A (**2**, t_R 58.3 min, 16.3 mg), respectively. Fractions AP and AS afforded hamigeran G (**8**, t_R 39.8 min, 22.0 mg) and hamigeran G enol (**9**, t_R 67.3 min, 4.8 mg).

The remaining amount of fraction D (approx. 1.5 g) was separated on LH-20 using 50% MeOH–CH_2Cl_2 as the running solvent. TLC and ^{1}H NMR analysis yielded a 185 mg hamigeran-enriched fraction, purified further using semi-preparative C18 HPLC (75–100% MeOH–0.2 M $HCOOH_{(aq)}$) into 15 fractions AX–BK. From this, 4-bromohamigeran K (**15**, t_R 79.9 min, 0.8 mg) was present in fraction BJ. Fractions AZ and BC were individually purified further using analytical C18 HPLC (70% MeOH–0.2 M $HCOOH_{(aq)}$) to give hamigeran L

(**16**, t_R 30.3 min, 4 mg) and hamigeran L 11-*O*-methyl ester (**17**, t_R 56.1 min, 1.4 mg), respectively.

Hamigeran K, 10-*epi*-hamigeran K and hamigeran A ethyl ester. A frozen sample of *Hamigera tarangaensis* (PTN2_79F, 25 g), collected from Cavalli Island, New Zealand, was extracted with EtOH (2 × 100 mL) and fractionated from PSDVB (30 mL, pre-equilibrated in EtOH) with 100 mL portions of (i) 20% Me_2CO–H_2O, (ii) 40% Me_2CO–H_2O, (iii) 60% Me_2CO–H_2O, (iv) 80% Me_2CO–H_2O and (v) Me_2CO. The 80% Me_2CO–H_2O fraction was separated on LH-20 using 50% EtOH–CH_2Cl_2 as the running solvent. Hamigeran-containing fractions, identified by TLC and ^{1}H NMR analysis, were pooled together and purified using semi-preparative C18 HPLC (75% MeOH–0.2 M $HCOOH_{(aq)}$) to give 13 fractions. Fraction 5 afforded hamigeran K (**13**, t_R 33.8 min, 0.5 mg), while fraction 8 was subjected to analytical (70% MeOH–0.2 M $HCOOH_{(aq)}$) C18 HPLC to give 10-*epi*-hamigeran K (**14**, t_R 69.9 min, 0.3 mg). Fraction 7 contained trace amounts of hamigeran A (**2**) observable by ^{1}H NMR. Fraction 10 afforded hamigeran A ethyl ester (**19**, t_R 59.1 min, 1.5 mg). A sample of the hamigeran-containing fraction from LH-20 purification was subjected to LCMS analysis (C18, 3.5 μ, 2.1 × 30 mm, 5–100% MeCN–0.5 mM $NH_4^+HCOO^-_{(aq)}$, 14.5 min ramp time), where hamigeran A (**2**, 9.8 min, $[M + Na]^+$, Δ = –1.7 ppm) and hamigeran A ethyl ester (**19**, 10.3 min, $[M + Na]^+$, Δ = +0.4 ppm) were detected.

Hamigeran A (2). Yellow film/needles; $[\alpha]_D^{25}$ −33° (*c* 1.1, CH_2Cl_2); UV (MeOH) λ_{max} 224 nm (ε 14 700), 282 nm (ε 9900), 344 nm (ε 4100); HRESIMS, $[M + Na]^+$, observed *m*/*z* 447.0786, calculated 447.0783 for $C_{20}H_{25}O_5{}^{79}BrNa$, Δ = +0.7 ppm; all other data as previously described.[2,16]

Debromohamigeran A (3). Pale yellow film; $[\alpha]_D^{25}$ −104° (*c* 0.09, CH_2Cl_2); UV (MeOH) λ_{max} 221 nm (ε 19 700), 278 nm (ε 16 000), 340 nm (ε 5800); HRESIMS, $[M + Na]^+$, observed *m*/*z* 369.1674, calculated 369.1678 for $C_{20}H_{26}O_5Na$, Δ = −1.1 ppm; all other data as previously described.[2]

Hamigeran B (4). Fine yellow needles; $[\alpha]_D^{25}$ −104° (*c* 0.9, CH_2Cl_2); UV (MeOH) λ_{max} 283 nm (ε 5300), 310 nm (ε 4600); HRESIMS, $[M + Na]^+$, observed *m*/*z* 387.0579, calculated 387.0572 for $C_{18}H_{21}O_3{}^{79}BrNa$, Δ = +1.8 ppm; all other data as previously described.[2]

Hamigeran F (6). Colourless film; $[\alpha]_D^{25}$ −21° (*c* 0.05, CH_2Cl_2); UV (HPLC, 85% MeOH–0.2 M $HCOOH_{(aq)}$) λ_{max} 220 nm (rel. int. 1), 337 nm (rel. int. 0.32); NMR data see Table 1; HRESIMS, $[M + Na]^+$, observed *m*/*z* 459.0781, calculated 459.0783 for $C_{21}H_{25}O_5{}^{79}BrNa$, Δ = −0.4 ppm.

Hamigeran F rearrangement product (7). Colourless film; $[\alpha]_D^{25}$ +76° (*c* 0.04, CH_2Cl_2); UV (MeOH) λ_{max} 228 nm (ε 9100), 273 nm (ε 4500), 338 nm (ε 2700); NMR data see ESI;† HRESIMS, $[M + Na]^+$, observed *m*/*z* 459.0776, calculated 459.0783 for $C_{21}H_{25}O_5{}^{79}BrNa$, Δ = −1.5 ppm.

Hamigeran G (8). Yellow film; $[\alpha]_D^{25}$ −131° (*c* 0.05, CH_2Cl_2); UV (MeOH) λ_{max} 272 nm (ε 2000), 327 nm (ε 2800); NMR data see Table 2 and ESI;† HRESIMS, $[M + Na]^+$, observed *m*/*z* 401.0734, calculated 401.0728 for $C_{19}H_{23}O_3{}^{79}BrNa$, Δ = +1.5 ppm.

Hamigeran H (10). Pale yellow film; $[\alpha]_D^{20}$ −70° (*c* 0.11, CH_2Cl_2); UV (MeOH) λ_{max} 230 nm (sh, ε 8500), 283 nm (ε 4500); NMR data see Table 2 and ESI;† HRESIMS, $[M + Na]^+$, observed *m*/*z* 397.1995, calculated 397.1991 for $C_{22}H_{30}O_5Na$, Δ = +1.0 ppm.

Hamigeran I (11). Pale yellow film; $[\alpha]_D^{18}$ −21° (*c* 0.04, CH_2Cl_2); UV (MeOH) λ_{max} 220 nm (ε 18 600), 280 nm (ε 6800); NMR data see Table 2 and ESI;† HRESIMS, $[M + Na]^+$, observed *m*/*z* 419.0837, calculated 419.0834 for $C_{19}H_{25}O_4{}^{79}BrNa$, Δ = +0.7 ppm.

Hamigeran J (12). Pale yellow film; $[\alpha]_D^{20}$ −5° (*c* 0.30, CH_2Cl_2); UV (MeOH) λ_{max} 230 nm (sh, ε 14 500), 289 nm (ε 5100); NMR data see Table 3 and ESI;† HRESIMS, $[M + Na]^+$, observed *m*/*z* 447.0786, calculated 447.0783 for $C_{20}H_{25}O_5{}^{79}BrNa$, Δ = +0.7 ppm.

Hamigeran K (13). Colourless film; $[\alpha]_D^{20}$ −9° (*c* 0.08, CH_2Cl_2); UV (MeOH) λ_{max} 225 nm (ε 16 300), 275 nm (ε 6900), 346 nm (ε 2600); NMR data see Table 3 and ESI;† HRESIMS, $[M + Na]^+$, observed *m*/*z* 389.0724, calculated 389.0728 for $C_{18}H_{23}O_3{}^{79}BrNa$, Δ = −1.0 ppm.

10-*epi*-Hamigeran K (14). Colourless film; $[\alpha]_D^{20}$ −14° (*c* 0.1, CH_2Cl_2); UV (MeOH) λ_{max} 226 nm (ε 15 200), 274 nm (ε 6300), 339 nm (ε 2700); NMR data see Table 3 and ESI;† HRESIMS, $[M + Na]^+$, observed *m*/*z* 389.0726, calculated 389.0728 for $C_{18}H_{23}O_3{}^{79}BrNa$, Δ = −0.5 ppm.

4-Bromohamigeran K (15). Colourless film; $[\alpha]_D^{25}$ +19° (*c* 0.05, CH_2Cl_2); UV (MeOH) λ_{max} 220 nm (ε 13 200), 279 nm (ε 2000), 350 nm (ε 1800); NMR data see Table 3 and ESI;† HRESIMS, $[M + Na]^+$, observed *m*/*z* 466.9833, calculated 466.9833 for $C_{18}H_{22}O_3{}^{79}Br_2Na$, Δ = 0.0 ppm.

Hamigeran L (16). Colourless film; $[\alpha]_D^{25}$ +66° (*c* 0.27, CH_2Cl_2); UV (MeOH) λ_{max} 218 nm (ε 29 400), 312 nm (ε 2500); NMR data see Table 2 and ESI;† HRESIMS, $[M + Na]^+$, observed *m*/*z* 435.0784, calculated 435.0783 for $C_{19}H_{25}O_5{}^{79}BrNa$, Δ = +0.2 ppm.

Hamigeran L 11-*O*-methyl ester (17). Colourless film; $[\alpha]_D^{25}$ +28° (*c* 0.09, CH_2Cl_2); UV (MeOH) λ_{max} 218 nm (ε 40 100), 308 nm (ε 3900); NMR data see Table 2 and ESI;† HRESIMS, $[M + Na]^+$, observed *m*/*z* 449.0933, calculated 449.0940 for $C_{20}H_{27}O_5{}^{79}BrNa$, Δ = −1.6 ppm.

12-Acetoxy-13-*epi*-neoverrucosan-5-one (18). Colourless film; $[\alpha]_D^{20}$ +11° (*c* 0.17, CH_2Cl_2); NMR data see ESI;† HRESIMS, $[M + Na]^+$, observed *m*/*z* 369.2401, calculated 369.2406 for $C_{22}H_{34}O_3Na$, Δ = −1.4 ppm.

Hamigeran A ethyl ester (19). Yellow film; $[\alpha]_D^{25}$ −57° (*c* 0.10, CH_2Cl_2); UV (MeOH) λ_{max} 226 nm (ε 8100), 282 nm (ε 3800), 351 nm (ε 1800); NMR data see ESI;† HRESIMS, $[M + Na]^+$, observed *m*/*z* 461.0932, calculated 461.0934 for $C_{21}H_{27}O_5{}^{79}BrNa$, Δ = −0.5 ppm.

Cell proliferation assays and chemical genomic screening

MTT cell proliferation assays were carried out in the promyelocytic leukaemic HL-60 cell line as previously described.[22] Chemical genomic screens for determining genetic interactions with hamigerans B and G in *S. cerevisiae* followed standard methods as described.[19,23]

Acknowledgements

The authors thank Yinrong Lu of Industrial Research Ltd, for running high-resolution mass spectra. Susann Scheunert, on internship from Georg Simon Ohm University of Applied Sciences, Nuremburg, Germany, is acknowledged for her assistance with hamigeran isolation. Victoria University of Wellington (A.J.S.), the Wellington Medical Research Foundation (J.H.M.) and the New Zealand Cancer Society (J.J.F., J.H.M.) are also acknowledged for funding.

Notes and references

1 R. C. Cambie, A. R. Lal, M. R. Kernan and P. R. Bergquist, *J. Nat. Prod.*, 1995, **58**, 940–942.
2 K. D. Wellington, R. C. Cambie, P. S. Rutledge and P. R. Bergquist, *J. Nat. Prod.*, 2000, **63**, 79–85.
3 R. C. Cambie, C. E. F. Rickard, P. S. Rutledge and K. D. Wellington, *Acta Crystallogr., Sect. C: Cryst. Struct. Commun.*, 2001, **57**, 958–960.
4 K. C. Nicolaou, D. Gray and J. Tae, *Angew. Chem., Int. Ed.*, 2001, **40**, 3675–3678.
5 K. C. Nicolaou, D. Gray and J. Tae, *Angew. Chem., Int. Ed.*, 2001, **40**, 3679–3683.
6 D. L. J. Clive and J. Wang, *Angew. Chem., Int. Ed.*, 2003, **42**, 3406–3409.
7 G. Mehta and H. M. Shinde, *Tetrahedron Lett.*, 2003, **44**, 7049–7053.
8 D. L. J. Clive and J. Wang, *J. Org. Chem.*, 2004, **69**, 2773–2784.
9 K. C. Nicolaou, D. L. F. Gray and J. Tae, *J. Am. Chem. Soc.*, 2004, **126**, 613–627.
10 B. M. Trost, C. Pissot-Soldermann, I. Chen and G. M. Schroeder, *J. Am. Chem. Soc.*, 2004, **126**, 4480–4481.
11 D. L. J. Clive and J. Wang, *Org. Prep. Proced. Int.*, 2005, **37**, 1–35.
12 C. E. Madu and C. J. Lovely, *Org. Lett.*, 2007, **9**, 4697–4700.
13 D. F. Taber and W. Tian, *J. Org. Chem.*, 2008, **73**, 7560–7564.
14 S. Y. W. Lau, *Org. Lett.*, 2011, **13**, 347–349.
15 P. R. Bergquist, *Sponges*, Hutchinson & Co., 1978.
16 The chemical shift of C-10 in our samples of hamigeran A consistently appears at δ_C 83.9, rather than δ_C 89.3 as originally reported in ref. 2.
17 D. J. Tantillo, *Nat. Prod. Rep.*, 2011, **28**, 1035–1053.
18 A. B. Parsons, A. Lopez, I. E. Givoni, D. E. Williams, C. A. Gray, J. Porter, G. Chua, R. Sopko, R. L. Brost, C. H. Ho, J. Wang, T. Ketela, C. Brenner, J. A. Brill, G. E. Fernandez, T. C. Lorenz, G. S. Payne, S. Ishihara, Y. Ohya, B. Andrews, T. R. Hughes, B. J. Frey, T. R. Graham, R. J. Andersen and C. Boone, *Cell*, 2006, **126**, 611–625.
19 P. Yibmantasiri, D. C. Leahy, B. P. Busby, S. A. Angermayr, A. G. Sorgo, K. Boeger, R. Heathcott, J. M. Barber, G. Moraes, J. H. Matthews, P. T. Northcote, P. H. Atkinson and D. S. Bellows, *Mol. BioSyst.*, 2012, **8**, 902–912.
20 H. E. Gottlieb, V. Kotlyar and A. Nudelman, *J. Org. Chem.*, 1997, **62**, 7512–7515.
21 P. R. Bergquist and P. J. Fromont, *The Marine Fauna of New Zealand: Porifera, Demospongiae, Part 4 (Poecilosclerida)*, New Zealand Oceanographic Institute, 1988.
22 K. J. Meyer, A. J. Singh, A. S. Tan, A. Cameron, D. C. Leahy, D. O'Sullivan, P. Joshi, A. C. La Flamme, P. T. Northcote, M. V. Berridge and J. H. Miller, *Mar. Drugs*, 2012, **10**, 900–917.
23 A. Wilmes, R. Hanna, R. Heathcott, P. T. Northcote, P. H. Atkinson, D. S. Bellows and J. H. Miller, *Gene*, 2012, **497**, 140–146.